Construction of a ceRNA regulatory network in Ziyang xiangcheng (Citrus junos Sieb. ex Tanaka) based on whole-genome transcriptome profiling of mRNAs, lncRNAs, miRNAs and circRNAs under Cu toxicity

Xing-zheng Fu (fuxingzheng@cric.cn)
Southwest University https://orcid.org/0000-0003-4088-6443
Xiao-Yong Zhang
Southwest University
Jie-Ya Qiu
Southwest University
Xue Zhou
Southwest University
Meng Yuan
Southwest University
Yi-Zhong He
Southwest University
Chang-Pin Chun
Southwest University
Li Cao
Southwest University
Li-Li Ling
Southwest University
Liang-Zhi Peng
Southwest University

Research article

Keywords: Citrus, Copper, CeRNA, Transcriptome, Non-coding RNA

Posted Date: August 22nd, 2019

DOI: https://doi.org/10.21203/rs.2.13386/v1

Version of Record: A version of this preprint was published on November 21st, 2019. See the published version at https://doi.org/10.1186/s12870-019-2087-1.

Abstract

Background Copper (Cu) toxicity has become a potential threat for citrus production, but little is known about related mechanisms. This study aims to uncover the global molecular response of mRNAs, long non-coding RNAs (lncRNAs), circular RNAs (circRNAs) and microRNAs (miRNAs) to Cu toxicity and to construct their competing endogenous RNAs (ceRNAs) network in citrus.Results In this study, tolerance of four commonly used rootstocks to Cu toxicity was first evaluated, and 'Ziyang Xiangcheng' (Citrus junos) was proved to be tolerant rootstock. Then the Cu-treated and -untreated root (CuR, CKR) and leaf (CuL, CKL) of 'Ziyang Xiangcheng' was selected to perform whole-genome transcriptome sequencing. In total, 5734 and 222 mRNAs, 164 and 5 lncRNAs, 45 and 17 circRNAs, and 147 and 130 miRNAs were identified to be differentially expressed (DE) in CuR/CKR and CuL/CKL, respectively. Gene ontology enrichment analysis of these DEmRNAs and targets of DElncRNAs and DEmiRNAs showed that most were annotated to oxidation-reduction, phosphorylation, membrane, and ion binding. The ceRNA network was constructed with the predicted DEmRNAs-DEmiRNAs and DElncRNAs-DEmiRNAs pairs, which further revealed regulatory roles of these DERNAs in Cu toxicity.Conclusions A large number of mRNAs, lncRNAs, circRNAs, and miRNAs were altered in response to Cu toxicity in citrus, and they may play crucial roles in mitigation of Cu toxicity through the ceRNA regulatory network.

Background

Copper (Cu) is an essential micronutrient for plant growth and development. As a redox-active transition element, Cu plays key roles in photosynthesis, respiration, C and N metabolism, oxidative stress protection, lignification, pollen fertility, and ethylene perception [1-4]. Most of the functions of Cu are based on enzymatically bound Cu, which catalyses redox reactions [1]. In plants, there are more than 100 Cu-containing proteins, such as plastocyanin (PC), copper/zinc superoxide dismutases (CSD), cytochrome c oxidase (COX), laccase (LAC), diamine oxidases (DAO), and polyphenol oxidases [1-3]. Despite being essential, Cu can easily be toxic to plants, even if its concentration only slightly rises to a supra-optimal level [5, 6]. Excess Cu inhibits plant growth and uptake of other mineral nutrients and alters enzyme systems, membrane integrity and many other biochemical and physiological processes[5]. Unfortunately, in the last decades, Cu contamination has become a global issue due to the long-term use of Cu-containing fungicides and bactericides, wastewater irrigation, and unconscionable Cu mining [6, 7]. In China, Cu is ranked as the fourth most contaminating heavy metal of agricultural lands [7, 8]. Thus, it is important to increase understanding of plant physiological and molecular responses to Cu stress.

Because Cu is both essential and toxic, plants have developed a tightly regulated homeostasis system to balance the uptake, efflux, chelation, distribution, and utilization of Cu [9, 10]. In this system, a number of functional proteins (such as Cu transporters and chaperones), transcription factors (TFs), as well as non-coding RNAs (ncRNAs) work together. Cu transporters including CTR-like Cu transporters (COPTs), P-type heavy metal ATPases (HMAs), yellow stripe-like (YSL) proteins, zinc/iron-regulated transporter (ZRT/IRT)-related proteins (ZIPs), and cation diffusion facilitators (CDFs) directly participate in Cu uptake, transport, and distribution [2, 3, 9, 11]. For example, the COPTs (such as COPT1, COPT2, and COPT6) are mainly responsible for Cu uptake from soil and redistribution to reproductive organs [12, 13]. The HMAs such as AtHMA5, AtHMA7/RAN1, AtHMA6/PAA1, and AtHMA8/PAA2 are involved in Cu transport into the xylem, chloroplast, or thylakoid in *Arabidopsis thaliana* [7, 14-16]. An YSL16 protein functions in recycling of Cu from older tissues to young tissues and grains [17]. Apart from these functional proteins, a conserved transcription factor called SPL7 (Squamosa Promoter binding-Like 7) has been shown to be a central regulator in Cu homeostasis [18, 19]. SPL7 regulates the expression of multiple targets that contain reiterative Cu-response elements (CuREs) with a GTAC motif in their promoters, such as COPT1, COPT2, COPT6, cupric reductases FRO4 and FRO5, and Cu-regulated microRNAs (miR397, miR398, miR408 and miR857), under Cu deficiency or excess [18, 20-22].

In addition to protein-coding RNAs, emerging evidence has revealed that ncRNAs also play essential regulatory roles in plant stress responses, including Cu stress [23]. MicroRNAs (miRNAs), one main class of ncRNA with a length of 19 to 24 nucleotides, participate in Cu homeostasis by repressing translation or directly degrading Cu-related proteins in plants [22, 24]. Previous studies found that Cu deficiency induced the expression of miR397, miR408, and miR857, which repressed a number of Cu-containing proteins such as CSD1, CSD2, LAC, COX subunit 5b (COX5b-1), and Cu chaperone for SOD (CCS1) [20, 25, 26], while Cu excess downregulated miR398 to induce the expression of CSD1 and CSD2 [27]. Recently, two new classes of ncRNA, namely, long non-coding RNAs (lncRNAs) and circular RNAs (circRNAs), were discovered in plants. LncRNAs belong a group of ncRNA longer than 200 nucleotides and can regulate the expression of genes through *cis-*/*trans*-acting or miRNA sponges [28, 29]. CircRNAs are a class of endogenous, covalently closed, circular RNAs generated by alternative circularization [30]. Increasing numbers of studies in animals, humans, and plants have proved that lncRNAs and circRNAs can act as competing endogenous RNAs (ceRNAs) to regulate a wide range of biological and developmental processes [31-37]. CeRNAs, including mRNAs, lncRNAs, circRNAs, and pseudogenes, are the transcripts that can competitive bind common miRNA response elements (MREs), and which are also named miRNA sponges to sequester specific miRNAs and suppress their function [30, 31, 34, 35]. Although no direct evidence has characterized the role of lncRNAs and circRNAs in Cu toxicity in plants, we can speculate it based on this ceRNA theory.

Citrus fruits are widely grown worldwide. With increasing environmental pollution such as the extensive usage of Cu-containing bactericides in controlling citrus canker disease in citrus production, Cu toxicity has become a threat for citrus. However, relevant research is greatly limited. To understand the underlying molecular mechanisms in response to Cu toxicity, a widely used citrus rootstock in China, Ziyang xiangcheng (*Citrus junos* Sieb. ex Tanaka), was chosen to perform deep RNAseq to reveal the differentially expressed profiles of mRNAs, lncRNAs, miRNAs, and circRNAs, and to uncover their ceRNA networks under Cu toxicity.

Methods

Plant materials and treatments

Seeds of four commonly used citrus rootstocks, trifoliate orange (*Poncirus trifoliata* L. Raf), 'Ziyang Xiangcheng' *(Citrus junos* Sieb. ex Tanaka), red tangerine (*Citrus reticulate* Blanco), and 'Shatian' pummelo (*Citrus grandis*) were collected from Citrus Research Institute, Southwest University, Chongqing, China. To evaluate the tolerance of four rootstocks to Cu toxicity, the seeds were germinated in plastic containers filled with quartz sand at a temperature of 28°C and a relative humidity of 80% for one to two weeks. Thereafter, uniform seedlings were transplanted into new quartz sand washed with distilled water at 25°C under a 16-h photoperiod (50 $\mu mol \cdot m^{-2} \cdot s^{-1}$) for sand culture. During sand culture, ½-strength Hoagland's solution composed of 4 mM $Ca(NO_3)_2$, 1.5 mM KNO_3, 0.5 mM $NH_4H_2PO_4$, 1 mM $MgSO_4$, 50 μM Fe-EDTA, 15 μM H_3BO_3, 10 μM $MnSO_4$, 5 μM $ZnSO_4$, 1.5 μM $CuSO_4$, and 1 μM H_2MoO_4, was irrigated every 4 days. After 30 d of growth, half of the seedlings were irrigated with the above normal solution (CK), while the others were irrigated with 187.5 μM $CuSO_4$ (125×) of ½-strength Hoagland's solution for 40 d of excess Cu treatment. Three biological replicates were performed for each treatment.

In the RNAseq experiment, seeds of 'Ziyang Xiangcheng' were first sterilized with 2% sodium hypochlorite for 15 min; then, the seed coats were removed, and seeds were germinated at a temperature of 28°C and a relative humidity of 80% for one week. Uniform seedlings were transferred to the above-mentioned normal ½-strength Hoagland's solution for hydroculture at 25°C under a 16-h photoperiod (50 $\mu mol \cdot m^{-2} \cdot s^{-1}$), and the solution was renewed every 10 d. After 30 d of growth, half of the seedlings were renewed with ½-strength Hoagland's solution containing 75 μM $CuSO_4$ (50×) for excess Cu treatment, while the others were renewed with normal solution (CK). After 1 d and 3 d of treatment, the roots and leaves of the seedlings were sampled, frozen in liquid nitrogen, and stored at −80°C. Three biological replicates were performed for each treatment.

Measurement of plant height growth rate and contents of chlorophyll and malonaldehyde

Plant height (PH) of the aerial part was measured with a ruler at 0 d (PH1) and 40 d of Cu treatment (PH2). The plant height growth rate was calculated as (PH2-PH1)×100/PH1%. The contents of chlorophyll and malonaldehyde (MDA) were determined as described by Fu et al [38].

RNA extraction, library preparation, and RNA sequencing

Total RNA was extracted from the roots and leaves of CK (abbreviated as CKR and CKL) and Cu-treated samples (abbreviated as CuR and CuL) using TRIzol Reagent (Invitrogen, Carlsbad, CA, USA) according to the manufacturer's protocol. RNA quality and integrity were estimated with an Agilent 2100 Bioanalyzer (Agilent Technologies, Santa Clara, CA, USA) and NanoDrop 2000 spectrophotometer (Thermo Scientific, Wilmington, DE, USA). Only high-quality RNA samples (1.8<OD260/280<2.2, OD260/230≥2.0, RIN≥7.0, 28S/18S≥1.0) were used to construct the sequencing library.

For mRNA, LncRNA, and circRNA sequencing, 5 μg of total RNA was used to prepare ribosomal RNA (rRNA) removed strand-specific library using a TruSeq Stranded Total RNA Library Prep with the Ribo-Zero Plant Kit (Illumina, San Diego, CA, USA) according to the manufacturer's instructions. There were three biological replicates per treatment, and a total of 12 libraries were prepared. For small RNA sequencing, 4 small RNA libraries were constructed with 3 μg of total RNA from CKL, CKR, CuL and CuR samples and the Truseq Small RNA sample prep Kit (Illumina, San Diego, CA, USA). After libraries were quantified by a TBS-380 Fluorometer (Turner Biosystem, Sunnyvale, CA, USA), deep RNA sequencing was performed using an Illumina HiSeq X Ten platform at Shanghai Majorbio Bio-Pharm Biotechnology Co. Ltd. (Shanghai, China).

Read mapping and transcriptome assembly

The paired-end raw reads were trimmed and quality controlled by SeqPrep (https://github.com/jstjohn/SeqPrep) and Sickle (https://github.com/najoshi/sickle) with default parameters. Then, clean reads were separately aligned to the Pummelo (*Citrus grandis*) genome [39] in orientation mode using Tophat2 software [40] (http://tophat.cbcb.umd.edu/). The mapped reads of each sample were assembled by Cufflink (http://cufflinks.cbcb.umd.edu/) in a reference-based approach.

Differentially expressed mRNA and gene ontology (GO) enrichment analysis

To identify differentially expressed mRNAs (DEmRNAs) between CK and Cu-treated samples, the expression level of each transcript was calculated according to the fragments per kilobase of exon per million mapped reads (FRKM) method. RSEM (http://deweylab.biostat.wisc.edu/rsem/) was used to quantify gene abundance [41]. R statistical package software EdgeR [42] was utilized for differential expression analysis with an absolute value of $\log_2$FC > 1 and FDR < 0.05. GO annotation and functional enrichment analysis of DEmRNAs were carried out using the Omicshare oneline platform (http://www.omicshare.com/tools/).

Identification of lncRNAs and prediction of their target genes

For identification of novel lncRNAs, the transcripts that overlapped with known protein-coding genes on the same strand, transcripts with a fragment count < 3, transcripts shorter than 200 nt, and an open reading frame (ORF) longer than 300 nt were first discarded. Then, we used the Coding Potential Calculator (CPC), Coding-Non-Coding index (CNCI), Coding Potential Assessment Tool (CPAT), and Pfam Scan to filter transcripts with coding potential. The overlapped outputs from CPC, CNCI, CPAT, and Pfam Scan were considered reliably expressed novel lncRNAs. We also refer to the lncRNAs in the GREENC database (http://greenc.sciencedesigners.com/wiki/Main_Page) as known lncRNAs. All identified lncRNAs were classified into intergenic, intronic, and antisense lncRNAs using the cuffcompare program in the Cufflinks suite. The expression level of each lncRNA was calculated according to the FRKM method. Differentially expressed lncRNAs (DELncRNAs) were extracted with an absolute value of $\log_2$FC > 1 and FDR < 0.05 by EdgeR. The potential *cis*- and *trans*-target mRNAs of DELncRNAs were predicted according to the position on the chromosome. The cis-targets were searched within a 10-kb window upstream or downstream of the lncRNA [43]. The *trans*-targets were predicted as described by Ou et al [44].

Identification and analysis of circRNAs

CircRNA Identifier (CIRI) and CIRCexplorer tools were used to identify circRNAs in this study. CIRI scans Sequence Alignment/Map (SAM) files and detects junction reads with paired chiastic clipping (PCC) signals and paired-end mapping (PEM) and GT-AG splicing signals as described by Gao et al [45]. CIRCexplorer obtains junction reads *via* a two-step TopHat and TopHat-Fusion mapping strategy as described by Zhang et al [46]. The overlapped outputs from CIRI and CIRCexplorer were used for further analysis. The expression level of each circRNA was calculated according to the Spliced Reads per Billion Mapping (SRPBM) method. Differentially expressed circRNAs (DEcircRNAs) were extracted with an absolute value of $\log_2$FC > 1 and FDR < 0.05 by DEGseq.

Identification and analysis of miRNAs

The raw data were first quality controlled with Fastx-toolkit software (http://hannonlab.cshl.edu/fastx_toolkit/) to obtain clean small RNA reads by filtering low-quality bases (Sanger base quality < 20), sequencing adapters, reads shorter than 18 nt, and reads longer than 32 nt. The assembled unique sequences with clean reads were then BLAST searched against the Rfam database (version 12.1, http://rfam.sanger.ac.uk/) to remove non-miRNA sequences (rRNA, tRNA, snoRNA, etc.). The remaining reads were used to predict known miRNAs through a BLAST search of the miRbase, version 21.0 (http://www.mirbase.org/), and novel miRNAs through analysis of the hairpin structure of the miRNA precursor with Mireap (http://sourceforge.net/projects/mireap) software. The expression level of each miRNA was calculated according to the transcripts per million reads (TPM) method. Differentially expressed miRNAs (DEmiRNAs) were extracted with an absolute value of $\log_2$FC > 1 and FDR < 0.005 by DEGseq. Target prediction of DEmiRNAs was performed with psRoboot [47].

Construction and analysis of ceRNAs regulatory network

To reveal the roles and interactions of lncRNAs, circRNAs, miRNAs, and mRNAs, we constructed an lncRNA-circRNA-miRNA-mRNA regulatory network based on the ceRNA hypothesis. psRobot [47] was used to predict the miRNA-lncRNA, miRNA-mRNA, and miRNA-circRNA pairs. The correlation between lncRNAs, circRNAs, miRNAs, and mRNAs was evaluated using the Pearson correlation coefficient (PCC) from matched pairs' expression profile data. The interaction network was built and visually displayed using Cytoscape software [48].

Quantitative real time PCR (qRT-PCR) validation of DEmRNAs, DElncRNAs, and DEmiRNAs

qRT-PCR was performed to validate the expression levels of DEmRNAs, DElncRNAs, and DEmiRNAs. Total RNA and small RNA were extracted from samples of CuR and CKR using an RNAprep pure Plant Kit (TIANGEN, Cat#DP432, China) and miRcute miRNA isolation kit (TIANGEN, Cat#DP501, China), respectively. First-strand cDNA was synthesized from 1 ug of total RNA with the HiScript® II Q RT SuperMix (Vazyme, Cat#R223, China) for qPCR of mRNA and with the lnRcute lncRNA First-Strand cDNA Synthesis Kit (TIANGEN, Cat#KR202, China) for qPCR of lncRNA. In addition, 1 μg of small RNA was used for cDNA synthesis using a miRNA 1st Strand cDNA Synthesis Kit (Vazyme, Cat#MR101, China) with the stem-loop primer designed by the stem-loop sequence (GTCGTATCCAGGGTCCGAGGTATTCGCACTGGATACGAC) except for the internal reference U6. qPCR was performed on the Bio-Rad CFX Connect RealTime system using ChamQ™ Universal SYBR® qPCR Master Mix (Vazyme, Cat#Q711), lnRcute lncRNA qPCR Detection Kit (TIANGEN, Cat#FP402) and miRNA Universal SYBR® qPCR Master Mix (Vazyme, Cat#MQ101) following the manufacturer's instructions. The $2^{-\Delta\Delta CT}$ method was used to normalize and determine the RNA level relative to an internal reference gene, actin (Cs1g05000.1) or U6. All primers are included in Additional file 9: Table S9.

Results

Tolerance evaluation of citrus rootstocks to Cu toxicity

To evaluate the tolerance of commonly used citrus rootstocks to Cu toxicity, trifoliate orange (TO), 'Ziyang Xiangcheng' (XC), red tangerine (RT), and 'Shatian' pummelo (ST) were subjected to excess Cu treatment. As shown in Fig. 1, after 25 d of treatment, top leaves of TO and ST showed a yellow color, while those of XC and RT were almost normal (similar to the phenotype of CK). Although the growth rate of plant height was significantly suppressed upon Cu toxicity, XC had a minimal impact among the four rootstocks. Chlorophyll contents were also significantly reduced upon Cu toxicity, but that in XC was obviously higher than that in TO, RT, and ST at 25 d and 40 d of treatment. In addition, excess Cu treatment resulted in a significant increase of MDA in TO, RT, and ST compared with CK, but increase of MDA in XC was inconspicuous. These results indicated that XC was the most tolerant to Cu toxicity among the tested rootstocks, followed by RT, while TO and ST were sensitive. Therefore, XC was selected to perform high-throughput RNA sequencing (RNAseq) for uncovering the underlying tolerant mechanisms.

mRNA expression profiles under Cu toxicity

Using pummelo as reference genome, we identified 30123 genes in leaves and roots of XC, and their log_2FC values are presented as Volcano Plot pictures in Fig. 2a and 2b, which ranged from -8.2 to 7.9 in roots and from -5.3 to 4.8 in leaves. Among all of these genes, 5734 (2162 up-regulated and 3572 down-regulated) and 222 (132 up-regulated and 90 down-regulated) DEmRNAs were identified in Cu-treated root (CuR/CKR) and leaf (CuL/CKL) groups, respectively (Fig. 2c and Additional file 1: Table S1). Moreover, 137 DEmRNAs were common between CuR/CKR and CuL/CKL. A heat map of DEmRNAs showed the general expression profiles of DEmRNAs in each treatment and also showed that the three repeats of each treatment always clustered together while the Cu-treated group and the CK group were clustered separately (Fig. 2d).

To explore the functions of the DEmRNAs, GO annotation and GO enrichment analysis were performed. As shown in Additional file 10: Fig. S1a and b, 12 GO terms under biological process (BP), 10 GO terms under cellular component (CC), and 9 GO terms under molecular function (MF) were annotated for DEmRNAs of the leaf, while 16 GO terms under BP, 11 GO terms under CC, and 13 GO terms under MF were annotated for DEmRNAs of the root. In both the leaf and root, most DEmRNAs were annotated to the metabolic process, single-organism process, localization process and response to stimulus under BP, to membrane, cell, organelle, and extracellular region under CC, and to binding, catalytic activity, transporter activity, antioxidant activity, transcription factor activity and nutrient reservoir activity under MF. In addition, signaling process, detoxification process, molecular transducer activity, and metallochaerone activity were annotated in the root specifically. GO enrichment analysis showed that significantly enriched GO terms in the leaf included the lignin catabolic process, phenylpropanoid catabolic process, apoplast region, golgi subcompartment, extracellular region, oxygen oxidoreductase activity, and peptidase regulator activity, while those in the root included the photosynthesis process, lignin catabolic process, microtubule-based movement process, oxidation-reduction process, phosphorylation process, MCM complex, photosystem I reaction center, extracellular region, membrane, dehydrogenase activity, peroxidase activity, protein kinase activity, iron ion binding, and heme binding (Fig. 2e and Additional file 10: Fig. S1c).

LncRNA expression profiles under Cu toxicity

In total, we identified 243 known lncRNAs and 1033 novel lncRNAs in the root and leaf of XC by blasting to known lncRNAs of citrus in the GREENC database and performing CNCI, CPC, CPAT and PfamScan analysis (Fig. 3a). Comparison of the genomic characterizations of the lncRNAs with mRNAs showed that their transcripts were similar in length distribution, except lncRNA had relative higher numbers of long transcripts (> 4500bp) than mRNA; for exon number, a higher percentage of lncRNAs had 2 to 4 exons; in addition, lncRNAs had a shorter ORF length and lower FPKM value (Fig. 3b–e). At a cutoff with an absolute value of log_2FC > 1 and FDR < 0.05, 164 (103 up-regulated and 61 down-regulated) and 5 (1 up-regulated and 4 down-regulated) DElncRNAs were identified in CuR/CKR and CuL/CKL groups, respectively (Fig. 3f and Additional file 2: Table S2). The log_2FC values of DElncRNAs ranged from -10.0 to 13.2 in the root, and -11.1 to 8.8 in the leaf. The general expression profiles of DElncRNAs are shown in Fig. 3g. Similar to DEmRNAs and DElncRNAs in the Cu-treated group and CK group were clustered separately, while their three repeats always clustered together.

To explore the potential functions of these DElncRNAs, their *cis*- and *trans*-targeted mRNAs were predicted with bioinformatics methods (Additional file 3: Table S3). GO annotation of the targets of DElncRNAs in the root showed that they were annotated in 16 GO terms under BP (mainly involved in metabolic process, cellular process, single-organism process, localization and response to stimulus), 13 GO terms under CC (mainly involved in membrane, cell, organelle and macromolecular complex), and 10 GO terms under MF (mainly involved in binding, catalytic activity, transporter activity, electron carrier activity, transcription factor activity, and antioxidant activity) (Additional file 11: Fig. S2). GO enrichment analysis of these targets showed that significantly enriched GO terms were the photosynthesis process, phosphorylation process, oxidation-reduction process, lignin catabolic process, phenylpropanoid catabolic process, MCM complex, photosystem I reaction center, extracellular region, membrane, dehydrogenase activity, peroxidase activity, protein kinase activity, iron ion binding, and heme binding (Fig. 3h).

CircRNA expression profiles under Cu toxicity

In total, 2404 circRNAs were identified in the leaf and root of XC, and 60.48%, 28.62%, and 10.90% of them belong to the intergenic region type, exon type, and intron type, respectively (Fig. 4c). The sequence length distribution of circRNAs is shown in Fig. 4a, and most of them were 10000 bp to 50000 bp, or shorter than 1200 bp. Chromosome 2 (chr2) included maximum circRNAs, followed by chr3, chr5, and chr8 (Fig. 4b). Log_2FC values of circRNAs are displayed in Fig. 4d and 4e, and 45 (28 up-regulated and 17 down-regulated) and 17 (11 up-regulated and 6 down-regulated) DEcircRNAs were identified in

CuR/CKR and CuL/CKL groups, respectively (Fig. 4f and Additional file 4: Table S4), among which, only 1 DEcircRNAs were common between CuR/CKR and CuL/CKL. A heat map showed the general expression profiles of DEcircRNAs in each treatment, and most DEcircRNAs were more highly expressed in the CuR group (Fig. 4g).

miRNA expression profiles under Cu toxicity

In the present study, a total of 23333512, 24526156, 21822295, and 25871923 raw reads were generated from CKL, CKR, CuL and CuR libraries, respectively. Of these raw reads, we obtained 15050388, 15173260, 13474928 and 13748074 clean reads after removing adaptor sequences, low-quality sequences, and reads shorter than 18 nt and longer than 32 nt. The lengths of most clean reads were 20–24 nt; most were 21 nt, followed by 24 nt (Fig. 5a). Small RNA classification showed that 81% of clean reads were rRNA (42%) and unmatched (39%), and there were also 14% miRNA, 5% tRNA, and 1% of other types (Fig. 5b). From 14% of clean reads, we finally identified 149 known miRNAs and 336 novel miRNAs. The top 10 expressed miRNAs in each sample are shown in Fig. 5c and 5d, and miR166a-3p and nov-m0105-3p exhibited the highest expression abundance. From known miRNAs 12 (10 up-regulated and 2 down-regulated) and 3 (all up-regulated) DEmiRNAs, and from novel miRNAs 135 (26 up-regulated and 109 down-regulated) and 127 (42 up-regulated and 85 down-regulated) DEmiRNAs were identified in CuR/CKR and CuL/CKL groups, respectively (Fig. 5e and 5f and Additional file 5: Table S5). The general expression profiles of these DEmiRNAs are shown in Fig. 5g and 5h. Their expression levels exhibited obvious differences between CK and Cu-treated samples and between root and leaf samples.

Targeted mRNAs of these DEmiRNAs are listed in Additional file 6: Table S6. We found that 84.7% of DEmRNAs in the leaf (188/222) and 81.0% of DEmRNAs in the root (4642/5734) were targeted by one or multiple DEmiRNAs. GO annotation of the targets of DEmiRNAs in the root showed that most of them were annotated to the metabolic process, cellular process, single-organism process, localization process, and response to stimulus under BP, to membrane, cell, organelle and macromolecular complex under CC, and to binding, catalytic activity and transporter activity under MF (Additional file 12: Fig. S3a and b). In addition, most targets of known DEmiRNAs were down-regulated. GO enrichment analysis showed that significantly enriched GO terms of targets of known DEmiRNAs in root were photosynthesis, microtubule-based movement, carbohydrate metabolic process, DNA polymerase complex, microtubule, membrane, cellulose synthase activity, microtubule binding, and catalytic activity, while those of novel DEmiRNAs were microtubule-based movement process, phosphorylation process, protein modification process, oxidation-reduction process, DNA polymerase complex, kinesin complex, extracellular region, membrane, protein kinase activity, transferase activity, anion binding, and catalytic activity (Fig. 6a and 6b).

CeRNA regulatory network in response to Cu toxicity

To reveal the global regulatory network of protein-coding RNAs and ncRNAs under Cu toxicity, a ceRNA network was constructed using DEmiRNAs, DEmRNAs, DElncRNAs, and DEcircRNAs based on ceRNA theory. In total, 5739 DEmRNAs, 64 DElncRNAs, and 5 DEcircRNAs were predicted as targets of 251 miRNAs in the root and leaf. When their correlation was further filtered with PCC > 0.8, we obtained 3819 DEmiRNA-DEmRNA and 10 DEmiRNA-DElncRNA interactions in the root and 12 DEmiRNA-DEmRNA interactions in the leaf (Fig. 7). In this ceRNA network, Nov-m0238-3p, Nov-m0074-5p, Nov-m0183-3p, miR166c-5p, Nov-m0128-3p, Nov-m0328-5p, miR165a-5p, and miR535c involved in more than 100 nodes and were considered the core regulators. In addition, lncRNAs including TCONS_00012501, TCONS_00012960, TCONS_00025983, TCONS_00027274, TCONS_00034874, TCONS_00036810, TCONS_00042747, TCONS_00051884 and TCONS_00062474 participated in the network.

Considering that the network contains enormous information and each one cannot be displayed in the figure, we constructed a mini-ceRNA network by reducing the mRNA amount. We identified 284 known Cu-related mRNAs that were reported directly or indirectly in previous literatures from all DEmRNAs of the root (Additional file 7: Table S7). The mini-ceRNA network was constructed with these 284 DEmRNAs and all DEmiRNAs, DElncRNAs, and DEcircRNAs. Finally, only 261 DEmiRNA-DEmRNA and 10 DEmiRNA-DElncRNA interactions (PCC > 0.8) containing 18 DEmiRNAs, 129 DEmRNAs, and 9 DElncRNAs were obtained and are displayed in Fig. 8. DEmiRNAs including miR166a-5p, miR395c, miR535c, miR395k, miR166c-5p, miR165a-5p, and miR399a were involved in more than 20 nodes, and all of them were up-regulated in the CuR. A known Cu-related key miRNA, miR398b, was identified in the network, which down-regulated and interacted with 5 DEmRNAs and 2 DElncRNAs. In addition, many known Cu-related key mRNAs such as SPL (Cg5g011720, Cg6g012520, Cg7g016770), YSL (Cg7g013630), HMA (Cg5g002920, Cg5g002930, Cg4g021370), ABC transporter (Cg5g018290, Cg5g027620, Cg3g011050, Cg3g009290, and Cg5g021160 etc.), LAC (Cg6g004840, Cg7g002640, Cg6g004880) and ZIP (Cg8g019240, Cg9g029160, Cg2g037280) were down-regulated in the network.

qRT-PCR validated mRNA-miRNA-LncRNA interactions under Cu toxicity

To confirm the results of RNAseq and validate predicted interactions of miRNA and their targets preliminarily, 6 miRNAs (miR398b, miR8175, miR157c-3p, miR166a-5p, miR165a-5p, and Nov-m0284-5p) and their targeted mRNAs and lncRNAs were selected from the ceRNA network to determine their expression levels by qRT-PCR. As shown in Table 1, qRT-PCR results agreed well with RNAseq data except several low-abundance mRNAs were undetectable. In addition, miRNA and its targets showed quite correct up- or down-regulated relationships. For example, miR398 was down-regulated and all of its predicted targets were up-regulated; miR8175 was up-regulated and all of its targets were down-regulated. This result not only suggests reliability of RNAseq data in this study, but also validates the constructed ceRNA network in a certain way.

Discussion

Although few Cu-responsive mRNAs or miRNAs have been identified in several kinds of plants, related studies are still insufficient. There is also a lack of direct evidence regarding whether or how lncRNAs and circRNAs are involved in Cu toxicity or deficiency in plants. In citrus, related studies are almost non-existent. We need to discover new players and uncover a global molecular regulatory network in plants in response to Cu stress. In this study, we utilized a whole-transcriptome RNAseq strategy for genome-wide screening of potential mRNA, miRNA, lncRNA, and circRNA candidates in response to Cu toxicity and to construct their ceRNA regulatory networks in citrus. These results provides abundant novel information for further uncovering Cu stress responsive mechanisms in both citrus and other plants.

Important mRNAs that respond to Cu toxicity in citrus

In this study, we identified 5734 DEmRNAs in the root upon 1 d of Cu treatment and 222 DEmRNAs in the leaf upon 3 d of Cu treatment. The numbers of DEmRNAs in the root were significantly higher than those in the leaf, suggesting that the root had dominant responses to Cu toxicity and which should be studied in particular. We also found that more DEmRNAs were down-regulated in the root but up-regulated in leaf. It is possible because the root mainly reduces uptake of Cu by down-regulating related genes under Cu excess, while the leaf mainly increases protection of cell integrity by up-regulating related genes[9,10].

To excavate essential mRNAs in response to Cu toxicity in citrus, we first searched 284 known Cu-related genes from a large number of DEmRNAs in the root; they included Cu-related regulators (SPL, YSL, CDPK, MAPK, and SUMO E3 Ligase, etc.), transporters (COPT, HMA, PPA, CDF, ZIP, OPT, and ABC transporter, etc.) and enzymes (LAC, CSD, CCS, PC, and COX, etc.) according to their functional description (Additional file 7: Table S7 and Additional file 8: Table S8). As stated in the Introduction, these genes play important roles in Cu stress. According to GO annotation analysis, there were 317 in response to stimulus, 596 in the membrane, 45 involved in antioxidant activity, 1 with metallochaperone activity, 32 with molecular transducer activity, 126 nucleic acid binding transcription factors, 18 with nutrient reservoir activity, 19 with receptor activity, and 188 with transporter activity in DEmRNAs in the root. It is well known that plant membrane proteins like transporters and receptors directly mediate transmembrane transport processes as well as perception and transduction of internal and external signals and function in uptake of nutrients and water[49]. Antioxidant activity and nutrient reservoir activity could play key roles in protection of cell integrity. Molecular transducer activity possible directly involves transduction of upstream signals, while the transcription factor is the important switch to control downstream gene expression under stress. Thus, we also considered these GO terms of DEmRNAs as important candidates in response to Cu toxicity. In addition, 137 mRNAs were commonly differentially expressed in CuR/CKR and CuL/CKL groups. These common DEmRNAs might participate in the basic response process under Cu toxicity. We also paid attention to DEmRNAs with a higher fold change of expression because higher expression of these mRNAs indicates a more intense response to Cu toxicity. Interestingly, from the top 20 $\log_2$FC of DEmRNAs, we found 4 egg cell-secreted proteins (Cg1g026400, Cg1g026630, Cg1g026360, Cg1g026610) that were significantly down-regulated. Sprunck et al.[50] reported in the Science journal that egg cell-secreted EC1 triggers sperm cell activation during double fertilization in *Arabidopsis thaliana (A. thaliana)*. Recently, Yan et al[4]. found that pollen fertility of *A. thaliana* requires Cu under regulation of SPL. Thus, we speculate that Cu toxicity may affect pollen fertilization by down-regulating the expression of SPL (all mRNAs descripted as SPL were down-regulated in this study) and egg cell-secreted protein in citrus. Overall, by combining all of these important known or predicted DEmRNAs, we finally obtained 1243 key candidates in response to Cu toxicity in citrus (as shown in Additional file 8: Table S8), and these ones will be primarily studied in future.

Important miRNAs in response to Cu toxicity in citrus

As expounded in several reviews, miRNAs mediate important regulatory processes under metal stress[20,22,24,51]. MiR397, miR398, miR408, and miR857 are the well characterized Cu miRNAs[22]. Particularly, miR398 was proved to significantly down-regulate under Cu excess[22,27,52]. In this study, we also identified miR398b exhibiting a similar result. In addition, several known DEmiRNAs including miR157c-3p, miR165a-5p, miR166a-5p, miR166c-5p, miR166e-5p, miR395c, miR395k, miR399a, miR535c, and miR8175 were significantly up-regulated in the root. Gielen et al. reported that miR157a, miR395b, and miR395c were up-regulated in the root or leaf of *A. thaliana* under Cu and cadmium (Cd) toxicity[53]. In a review summarized by Gupta et al., miR157, miR166 and miR399 were shown to play important roles in manganese (Mn), Cd, arsenic (As) or aluminum (Al) toxicity[51]. Although no direct evidence has proved the function of miR535 in metal stress, its same superfamily and high sequence similarity of miRNA, miR156 has been well documented in Cd, Al, Mn, and As toxicity by targeting SPL genes[51,54]. Based on these previous studies, we can predict an important function of these known DEmiRNAs under Cu toxicity. Apart from known DEmiRNAs, we also identified more than 100 novel DEmiRNAs. Some of them such as Nov-m0238-3p, Nov-m0074-5p, Nov-m0183-3p, Nov-m0128-3p, and Nov-m0328-5p targeted dozens of DEmRNAs and DElncRNAs and were located in the center of the ceRNA network and should be also considered important candidates in response to Cu toxicity in citrus.

Possible function of lncRNA and circRNA in citrus Cu toxicity

LncRNA and circRNA have recently become a hot research field because they have been increasingly identified in various kinds of plants, and they are also widely recognized to play important functions in transcriptional and post-transcriptional regulation[55]. In this study, we identified 1276 lncRNAs (243 known

lncRNAs and 1033 novel lncRNAs) and 2404 circRNAs in XC by deep RNAseq. Previous studies have shown that the number of lncRNAs appeared to be positively correlated with the number of protein-coding genes, while the number of circRNAs depended on different species, treatments, and developmental stages[55,56]. A survey of 10 plants by Deng et al.[56] found that the number of lncRNAs varied from 2986 (*A. thaliana*) to 18031 (maize). Moreover, He et al.[57] identified 2085 lncRNAs in cucumber, and Feng et al.[58] identified 2546 lncRNAs in *Brassica napus*. The number of lncRNAs often ranges from thousands to tens of thousands in plants[55]. Recently, Zhao et al.[59] summarized the present scenario of circRNAs in plants. Abundant circRNAs have been identified in rice, *A. thaliana*, barley, tomato, wheat, soybean, maize, kiwifruit, etc. by high-throughput sequencing, of which the number varied from tens to tens of thousands[59]. In citrus, we only found that Ke et al.[60] identified 1238 (*Citrus paradisi*) to 3285 (*Atalantia buxifolia*) lncRNAs in nine citrus species, and Wang et al.[61] identified a total of 6584 potential lncRNAs in trifoliate orange. In addition, Zeng et al.[62] identified 558 potential circRNAs in trifoliate orange. Apart from these previous studies, our data provide new information on lncRNAs and circRNAs for another important citrus species, XC.

Regarding the function of plant lncRNAs and circRNAs, a large number of studies show that they play vital roles in stress responses[23,28,55,59]. For example, Franco-Zorrilla et al.[63] overexpressed an lncRNA IPS1 in *A. thaliana,* resulting in increased accumulation of the miR-399 targeted PHO2, which functions in phosphate uptake. In *Brassica napus*, 301 lncRNAs were identified as Cd stress responsive by high-throughput sequencing[58]. In rice, a large number of lncRNAs were identified to be induced by phosphate starvation or Cd stress[32,64]. In *Populus*, 126 lncRNAs were significantly altered under low-N stress[65]. Recently, Zhu et al.[66] identified 1934 circRNAs in the root and 44 in the leaf in response to salt stress in cucumber. Ren et al.[67] identified 23 circRNAs that were involved in the regulation of low nitrogen-promoted root growth in wheat, and Pan et al.[68] uncovered 1583 heat-specific circRNAs by RNAseq and bioinformatic analysis in *A. thaliana*. In this study, we identified 168 lncRNAs and 61 circRNAs responsive to Cu stress in the root and leaf of XC. To the best of our knowledge, this is possibly the first identification of Cu-responsive lncRNAs and circRNAs in plants. Based on ceRNA theory , we speculate that these lncRNAs and circRNAs are involved in Cu stress possible through competitive binding Cu-responsive miRNAs[31,55]. Next, we need to characterize the detailed mechanisms by which lncRNA and circRNA function in citrus Cu stress.

Proposed model in response to Cu toxicity based on ceRNA network

The ceRNA hypothesis is now widely accepted since it was reported several years ago[31]. In several studies of plants, ceRNA regulatory theory has been used to uncover molecular mechanisms of biology. For example, Xu et al.[32] constructed a ceRNA network to explain the function of lncRNAs in phosphate starvation of rice. Zhu et al.[33] reported a complex ceRNA network consisting of lncRNAs, mRNAs, and miRNAs in maize seed development. A large number of circRNAs was found in the ethylene pathway of tomato, possibly acting as ceRNAs[69]. Recently, a ceRNA network was also reported in *A. thaliana* leaf development, tomato flowering, and cucumber heat stress[35,37,39,57]. Our study constructed a possible ceRNA regulatory network in response to citrus Cu toxicity, which described the global molecular network among mRNAs, miRNAs, and lncRNAs.

Based on the ceRNA network, other results obtained in this study and references, a model of mRNA, miRNA, lncRNA, circRNA in response to Cu toxicity was proposed in Fig. 9. Under Cu toxicity, miRNAs act as the key regulators that directly target important Cu transporters, Cu proteins and Cu regulators (TFs and kinases) to regulate the uptake, efflux and distribution of Cu and to increase protection of cell integrity. In this process, some lncRNAs can act as ceRNA to competitively bind the MRE of miRNAs, which may indirectly affect the expression of mRNA. Moreover, circRNAs possible act as another type of ceRNA to sequester Cu-responsive miRNAs and suppress their function because many DEcircRNAs in response to Cu toxicity were identified in this study, although there was somewhat unexpected that circRNAs were not included in the ceRNA network. Regarding why circRNAs are not in ceRNA network, we analyze the reason is possible that the network was constructed under the strict filter criteria in predicting ceRNA pairs and interactions between significantly differentially expressed RNAs. We also find that most of DElncRNAs were not included in the ceRNA network. These lncRNAs are involved in Cu toxicity possible through other different mechanisms. For example, lncRNAs can be transcribed as miRNA precursors, induce DNA methylation, mediate chromatin modification, and act as transcriptional enhancers as reviewed by Hou et al[55]. Overall, the expression of a large number of mRNAs, lncRNAs, circRNAs and miRNAs were altered in response to Cu toxicity in citrus, and they may work synergistically or antagonistically to alleviate Cu toxicity through the ceRNA regulatory network.

Conclusions

Tolerance evaluation showed that XC was a tolerant rootstock to Cu toxicity. Whole-transcriptome RNAseq helped us to identify 5734 (2162 up-regulated and 3572 down-regulated) and 222 (132 up-regulated and 90 down-regulated) DEmRNAs in CuR/CKR and CuL/CKL groups, respectively. Of these, 1243 were considered key candidates in response to excessive Cu. We also identified 243 known lncRNAs and 1033 novel lncRNAs, of which 164 (103 up-regulated and 61 down-regulated) and 5 (1 up-regulated and 4 down-regulated) were significantly differentially expressed in CuR/CKR and CuL/CKL groups, respectively. From 2404 identified circRNAs, only 45 (28 up-regulated and 17 down-regulated) and 17 (11 up-regulated and 6 down-regulated) DEcircRNAs were identified in CuR/CKR and CuL/CKL groups, respectively. In addition, 149 known miRNAs and 336 novel miRNAs were predicted in XC, and 147 and 130 of them were responsive to Cu toxicity in the root and leaf, respectively. GO enrichment analysis of these DEmRNAs and targets of DElncRNAs and DEmiRNAs showed that most were annotated to oxidation-reduction, phosphorylation, membrane, and ion binding. A ceRNA network consisting of differentially expressed mRNAs, miRNAs, and lncRNAs was also constructed, which further revealed the critical roles of these DERNAs in citrus Cu toxicity.

Abbreviations

lncRNAs: long non-coding RNAs; circRNAs: circular RNAs; miRNAs: microRNAs; ceRNAs: competing endogenous RNAs; DE: differentially expressed; RNAseq: RNA sequencing; XC: 'Ziyang Xiangcheng'; FC: fold change; GO: gene ontology; MDA: malonaldehyde; BP: biological process; CC: cellular component; MF: molecular function; FRKM: the fragments per kilobase of exon per million mapped reads; CPC: coding potential calculator; CNCI: coding-non-coding index; CPAT: coding potential accessment tool

Declarations

Ethics approval and consent to participate

Not applicable.

Consent for publication

Not applicable.

Availability of data and material

All supporting data can be found within the manuscript and its additional supporting files.

Competing interests

The authors declare that they have no competing interests

Funding

This work was financially supported by the National Key Research and Development Program of China (2018YFD1000300, 2017YFD0202000), the National Natural Science Foundation of China (31772280), and the National Citrus Engineering Research Center (NCERC2019001). The funders provided the financial support to the RNAseq, but didn't play role in in the design of the study, collection, analysis, interpretation of data, and in writing the manuscript.

Authors' contributions

XZF and LZP conceived and designed the study. XZF, XYZ, and YZH analyzed the data. JYQ and XZ performed qRT-PCR. MY and LC prepared experimental materials. CPC and LLL measured physiological data. XZF wrote the paper. All authors read and approved the final manuscript.

Acknowledgements

Not applicable.

References

1. Broadley M, Brown P, Cakmak I, Rengel Z, Zhao F. Function of nutrients: Micronutrients. p. 191-248. In: P. Marschner (eds.), Mineral Nutrition of Higher Plants, Elsevier, 2012.
2. Burkhead JL, Reynolds KAG, Abdel-Ghany SE, Cohu CM, Pilon M. Copper homeostasis. New Phyt. 2009;182:799-816.
3. Yruela, I. Copper in plants: acquisition, transport and interactions. Funct Plant Biol. 2009;36:409-430.
4. Yan JP, Chia JC, Sheng HJ, Jung HI, Zavodna TO, Zhang L, Huang R, Jiao C, Craft EJ, Fei ZJ *et al*. Arabidopsis pollen fertility requires the transcription factors CITF1 and SPL7 that regulate copper delivery to anthers and jasmonic acid synthesis. Plant Cell 2017;29:3012-3029.
5. Cambrolle J, Garcia JL, Figueroa ME, Cantos M. Evaluating wild grapevine tolerance to copper toxicity. Chemosphere 2015;120:171-178.
6. Leng XP, Jia HF, Sun X, Shangguan LF, Mu Q, Wang BJ, Fang JG. Comparative transcriptome analysis of grapevine in response to copper stress. Sci Rep. 2015;5: 17749.
7. Huang XY, Deng FL, Yamaji N, Pinson SRM, Fujii-Kashino M, Danku J, Douglas A, Guerinot ML, Salt DE, Ma JF. A heavy metal P-type ATPase OsHMA4 prevents copper accumulation in rice grain. Nat Commun. 2016;7: 12138.
8. Zhao FJ, Ma YB, Zhu YG, Tang Z, McGrath SP. Soil contamination in China: current status and mitigation strategies. Environ Sci Technol. 2015;49:750-759.
9. Clemens S. Molecular mechanisms of plant metal tolerance and homeostasis. Planta 2001; 212:475-486.
10. Clemens S, Palmgren MG, Kramer U. A long way ahead: understanding and engineering plant metal accumulation. Trends Plant Sci. 2002;7:309-315.
11. Aguirre G, Pilon M. Copper delivery to chloroplast proteins and its regulation. Front Plant Sci. 2016; 6:1250.
12. Sancenon V, Puig S, Mateu-Andres I, Dorcey E, Thiele DJ, Penarrubia L. The Arabidopsis copper transporter COPT1 functions in root elongation and pollen development. J Biol Chem. 2004;279:15348-15355.
13. Jung HI, Gayomba SR, Rutzke MA, Craft E, Kochian LV, Vatamaniuk OK. COPT6 is a plasma membrane transporter that functions in copper homeostasis in Arabidopsis and is a novel target of SQUAMOSA promoter-binding protein-like 7. J Biol Chem. 2012;287:33252-33267.

14. Andres-Colas N, Sancenon V, Rodriguez-Navarro S, Mayo S, Thiele DJ, Ecker JR, Puig S, Penarrubia L. The Arabidopsis heavy metal P-type ATPase HMA5 interacts with metallochaperones and functions in copper detoxification of roots. Plant J. 2006;45:225-236.
15. Shikanai T, Muller-Moule P, Munekage Y, Niyogi KK, Pilon M. PAA1, a P-type ATPase of Arabidopsis, functions in copper transport in chloroplasts. Plant Cell 2003;15:1333-1346.
16. Abdel-Ghany SE, Muller-Moule P, Niyogi KK, Pilon M, Shikanai T. Two P-type ATPases are required for copper delivery in Arabidopsis thaliana chloroplasts. Plant Cell 2005;17:1233-1251.
17. Zheng LQ, Yamaji N, Yokosho K, Ma JF. YSL16 is a phloem-localized transporter of the copper-nicotianamine complex that is responsible for copper distribution in rice. Plant Cell 2012;24:3767-3782.
18. Yamasaki H, Hayashi M, Fukazawa M, Kobayashi Y, Shikanai T. SQUAMOSA promoter binding protein-like 7 is a central regulator for copper homeostasis in Arabidopsis. Plant Cell 2009;21:347-361.
19. Araki R, Mermod M, Yamasaki H, Kamiya T, Fujiwara T, Shikanai T. SPL7 locally regulates copper-homeostasis-related genes in Arabidopsis. J Plant Physiol. 2018;224:137-143.
20. Yamasaki H, Abdel-Ghany SE, Cohu CM, Kobayashi Y, Shikanai T, Pilon M. Regulation of copper homeostasis by micro-RNA in Arabidopsis. J Biol Chem. 2007;282:16369-16378.
21. Bernal M, Casero D, Singh V, Wilson GT, Grande A, Yang HJ, Dodani SC, Pellegrini M, Huijser P, Connolly EL, Merchant SS, Kramer U. Transcriptome sequencing identifies SPL7-regulated copper acquisition genes FRO4/FRO5 and the copper dependence of iron homeostasis in Arabidopsis. Plant Cell 2012;24:738-761.
22. Pilon M. The copper microRNAs. New Phyt. 2017;213:1030-1035.
23. Wang JJ, Meng XW, Dobrovolskaya OB, Orlov YL, Chen M. Non-coding RNAs and their roles in stress response in plants. Genom Proteom Bioinf 15, 301-312 (2017).
24. Chien PS, Chiang CB, Wang ZR, Chiou TJ. MicroRNA-mediated signaling and regulation of nutrient transport and utilization. Curr Opin Plant Biol 39, 73-79 (2017).
25. Abdel-Ghany SE, Pilon M. MicroRNA-mediated systemic down-regulation of copper protein expression in response to low copper availability in Arabidopsis. J Biol Chem 283, 15932-15945 (2008).
26. Lu SF, Li QZ, Wei HR, Chang MJ, Tunlaya-Anukit S, Kim H, Liu J, Song JY, Sun YH, Yuan LC *et al*. Ptr-miR397a is a negative regulator of laccase genes affecting lignin content in Populus trichocarpa. P Natl Acad Sci USA 110, 10848-10853 (2013).
27. Sunkar R, Kapoor A, Zhu JK. Posttranscriptional induction of two Cu/Zn superoxide dismutase genes in Arabidopsis is mediated by downregulation of miR398 and important for oxidative stress tolerance. Plant Cell 18, 2051-2065 (2006).
28. Chekanova JA. Long non-coding RNAs and their functions in plants. Curr Opin Plant Biol 27, 207-216 (2015).
29. Ma KS, Shi WS, Xu MY, Liu JX, Zhang FX. Genome-wide identification and characterization of long non-coding RNA in Wheat roots in response to Ca^{2+} channel blocker. Front Plant Sci 9, 244 (2018).
30. Li QF, Zhang YC, Chen YQ, Yu Y. Circular RNAs roll into the regulatory network of plants. Biochem Bioph Res 488, 382-386 (2017).
31. Salmena L, Poliseno L, Tay Y, Kats L, Pandolfi PP. A ceRNA hypothesis: the Rosetta Stone of a hidden RNA language? Cell 146, 353-358 (2011).
32. Xu XW, Zhou XH, Wang RR, Peng WL, An Y, Chen LL. Functional analysis of long intergenic non-coding RNAs in phosphate-starved rice using competing endogenous RNA network. Sci Rep 6, 20715 (2016).
33. Zhu M, Zhang M, Xing LJ, Li WZ, Jiang HY, Wang L, Xu MY. Transcriptomic analysis of long non-coding RNAs and coding genes uncovers a complex regulatory network that is involved in maize seed development. Genes-Basel 8 (2017).
34. Ren GJ, Fan XC, Liu TL, Wang SS, Zhao GH. Genome-wide analysis of differentially expressed profiles of mRNAs, lncRNAs and circRNAs during Cryptosporidium baileyi infection. BMC Genomics 19, 356 (2018).
35. Meng XW, Zhang PJ, Chen Q, Wang JJ, Chen M. Identification and characterization of ncRNA-associated ceRNA networks in Arabidopsis leaf development. BMC Genomics 19, 607 (2018).
36. Yuan Y, Li JM, Xiang W, Liu YH, Shu J, Gou ML, Qing M. Analyzing the interactions of mRNAs, miRNAs, lncRNAs and circRNAs to predict competing endogenous RNA networks in glioblastoma. J Neuro-Oncol 137, 493-502 (2018).
37. Yang ZC, Yang CC, Wang ZY, Yang Z, Chen DY, Wu YJ. LncRNA expression profile and ceRNA analysis in tomato during flowering. Plos One 14, e0210650 (2019).
38. Fu XZ, Khan EU, Hu SS, Fan QJ, Liu JH. Overexpression of the betaine aldehyde dehydrogenase gene from *Atriplex hortensis* enhances salt tolerance in the transgenic trifoliate orange (*Poncirus trifoliata* L. Raf.). Environ Exp Bot 74, 106-113 (2011).
39. Wang X, Xu YT, Zhang SQ, Cao L, Huang Y, Cheng JF, Wu GZ, Tian SL, Chen CL, Liu Y *et al*. Genomic analyses of primitive, wild and cultivated citrus provide insights into asexual reproduction. Nat Genet 49, 765-772 (2017).
40. Kim, D. et al. TopHat2: accurate alignment of transcriptomes in the presence of insertions, deletions and gene fusions. Genome Biol 14, R36 (2013).
41. Li B, Dewey CN. RSEM: accurate transcript quantification from RNA-Seq data with or without a reference genome. BMC Bioinformatics 12, 323 (2011).
42. Robinson MD, McCarthy DJ, Smyth GK. EdgeR: a Bioconductor package for differential expression analysis of digital gene expression data. Bioinformatics 2010;26:139-140.

43. Jia H, Osak M, Bogu GK, Stanton LW, Johnson R, Lipovich L. Genome-wide computational identification and manual annotation of human long noncoding RNA genes. RNA 2010;16:1478-1487.
44. Ou LJ, Liu ZB, Zhang ZQ, Wei G, Zhang YP, Kang LY, Yang BZ, Yang S, Lv JH, Liu YH *et al*. Noncoding and coding transcriptome analysis reveals the regulation roles of long noncoding RNAs in fruit development of hot pepper (Capsicum annuum L.). Plant Growth Regul. 2017; 83:1-16.
45. Gao Y, Wang JF, Zhao FQ. CIRI: an efficient and unbiased algorithm for de novo circular RNA identification. Genome Biol. 2015;16:4.
46. Zhang XO, Wang HB, Zhang Y, Lu XH, Chen LL, Yang L. Complementary sequence-mediated exon circularization. Cell 2014;159:134-147.
47. Wu HJ, Ma YK, Chen T, Wang M, Wang XJ. PsRobot: a web-based plant small RNA meta-analysis toolbox. Nucleic Acids Res. 2012;40:W22-28.
48. Shannon P, Markiel A, Ozier O, Baliga NS, Wang JT, Ramage D, Amin N, Schwikowski B, Ideker T. Cytoscape: a software environment for integrated models of biomolecular interaction networks. Genome Res. 2003;13:2498-2504.
49. Liu CL, Shen WJ, Yang C, Zeng LZ, Gao CJ. Knowns and unknowns of plasma membrane protein degradation in plants. Plant Sci. 2018;272:55-61.
50. Sprunck S, Rademacher S, Vogler F, Gheyselinck J, Grossniklaus U, Dresselhaus T. Egg cell-secreted EC1 triggers sperm cell activation during double fertilization. Science 2012;338:1093-1097.
51. Gupta OP, Sharma P, Gupta RK, Sharma I. MicroRNA mediated regulation of metal toxicity in plants: present status and future perspectives. Plant Mol Biol. 2014;84:1-18.
52. Leng XP, Wang PP, Zhao PC, Wang MQ, Cui LW, Shangguan LD, Wang C. Conservation of microRNA-mediated regulatory networks in response to copper stress in grapevine. Plant Growth Regul. 2017;82:293-304.
53. Gielen H, Remans T, Vangronsveld J, Cuypers A. Toxicity responses of Cu and Cd: The involvement of miRNAs and the transcription factor SPL7. BMC Plant Biol. 2016;16:145.
54. Ding YF, Chen Z, Zhu C. Microarray-based analysis of cadmium-responsive microRNAs in rice (*Oryza sativa*). J Exp Bot. 2011;62:3563-3573.
55. Hou JN, Lu DD, Mason AS, Li BQ, Xiao ML, An SF, Fu DH. Non-coding RNAs and transposable elements in plant genomes: emergence, regulatory mechanisms and roles in plant development and stress responses. Planta 2019;50:23-40.
56. Deng PC, Liu S, Nie XJ, Weining S, Wu L. Conservation analysis of long non-coding RNAs in plants. Sci China Life Sci. 2018;61:190-198.
57. He X, Guo S, Wang Y, Wang L, Shu S, Sun J (2019). Systematic identification and analysis of heat-stress-responsive lncRNAs, circRNAs and miRNAs with associated co-expression and ceRNA networks in cucumber (*Cucumis sativus* L.). Physiol Plantarum 10.1111/ppl.12997 (2019).
58. Feng SJ, Zhang XD, Liu XS, Tan SK, Chu SS, Meng JG, Zhao KX, Zheng JF, Yang ZM. Characterization of long non-coding RNAs involved in cadmium toxic response in *Brassica napus*. Rsc Adv. 2016;6:82157-82173.
59. Zhao W, Chu SS, Jiao YQ. Present scenario of circular RNAs (circRNAs) in plants. Front Plant Sci. 2019;10:379.
60. Ke LL, Zhou ZW, Xu XW, Wang X, Liu YL, Xu YT, Huang Y, Wang ST, Deng XX, Chen LL *et al*. Evolutionary dynamics of lincRNA transcription in nine citrus species. Plant J. 2019;98:912-927.
61. Wang CY, Liu SR, Zhang XY, Ma YJ, Hu CG, Zhang JZ. Genome-wide screening and characterization of long non-coding RNAs involved in flowering development of trifoliate orange (*Poncirus trifoliata* L. Raf.). Sci Rep. 2017;7:43226.
62. Zeng RF, Zhou JJ, Hu CG, Zhang JZ. Transcriptome-wide identification and functional prediction of novel and flowering-related circular RNAs from trifoliate orange (*Poncirus trifoliata* L. Raf.). Planta 2018;47:1191-1202.
63. Franco-Zorrilla JM, Valli A, Todesco M, Mateos I, Puga MI, Rubio-Somoza I, Leyva A, Weigel D, Garcia JA, Paz-Ares J. Target mimicry provides a new mechanism for regulation of microRNA activity. Nat Genet. 2007;39:1033-1037.
64. Chen, L. et al. Genome-wide analysis of long non-coding RNAs affecting roots development at an early stage in the rice response to cadmium stress. BMC Genomics 19, 460 (2018).
65. Chen L, Shi SL, Jiang NF, Khanzada H, Wassan GM, Zhu CL, Peng XS, Xu J, Chen YJ, Yu QY *et al*. Genome-wide identification and characterization of novel lncRNAs in Populus under nitrogen deficiency. Mol Genet Genomics 2016;291:1663-1680.
66. Zhu YX, Jia JH, Yang L, Xia YC, Zhang HL, Jia JB, Zhou R, Nie PY, Yin JL, Ma DF *et al*. Identification of cucumber circular RNAs responsive to salt stress. BMC Plant Biol. 2019;19:164.
67. Ren YZ, Yue HF, Li L, Xu YH, Wang ZQ, Xin ZY, Lin TB. Identification and characterization of circRNAs involved in the regulation of low nitrogen-promoted root growth in hexaploid wheat. Biol Res. 2018;51:43.
68. Pan T, Sun XQ, Liu YX, Li H, Deng GB, Lin HH, Wang SH. Heat stress alters genome-wide profiles of circular RNAs in Arabidopsis. Plant Mol Biol. 2018; 96:217-229.
69. Wang YX, Wang Q, Gao LP, Zhu BZ, Luo YB, Deng ZP, Zuo JH. Integrative analysis of circRNAs acting as ceRNAs involved in ethylene pathway in tomato. Physiol Plantarum 2017;161:311-321.

Tables

RNA	log_2FC(CuR/CKR) by RNAseq	log_2FC(CuR/CKR) by qPCR	*A. thaliana* description
miR398b	**-1.72561**	**-1.22962**	
TCONS_00012501	3.6	4.77311	
TCONS_00012960	1.32	1.392306	
Cg6g016060	3.06	3.721868	ABC transporter G family member 39
Cg1g001620	2.35	2.21382	Oligopeptide transporter 7
Cg1g015400	4.19	3.447331	Multicopper oxidase LPR1
Cg5g003300	1.76	1.164213	ABC transporter A family member 7
Cg8g024350	1.82	undetected	Mitogen-activated protein kinase kinase 14
miR8175	**1.089447**	**1.058019**	
Cg6g001870	-1.02	undetected	Laccase-11
Cg4g001090	-2.13	-1.88539	Protein TIC 55, chloroplastic
Cg9g027310	-2.25	-2.70294	Detoxifying efflux carrier 35
Cg2g021840	-2.35	-4.28181	Cyclic nucleotide-gated ion channel 4
Cg6g016050	-2.39	-1.89089	ABC transporter G family member 34
Cg2g047100	-2.4	-2.92599	Ferric reduction oxidase 7
Cg7g023310	-2.83	-2.96635	MATE efflux family protein 1
Cg2g001540	-3.09	-4.80108	Transducin/WD40 repeat-like superfamily protein
Cg6g005760	-4.11	-4.6826	Copper transporter 1
miR157c-3p	**1.98457**	**1.730227**	
Cg5g033620	-1.1	-2.39108	E3 ubiquitin-protein ligase BAH1
Cg6g020410	-1.21	-1.88539	ABC transporter G family member 14
Cg5g026950	-1.23	undetected	RING/U-box superfamily protein
Cg6g016780	-1.54	-2.09326	RCC1family with FYVE zinc finger domain
Cg5g011170	-1.72	-1.56999	Chaperone protein ClpB1
Cg7g023250	-1.76	-1.79581	E3 ubiquitin ligase BIG BROTHER
Cg9g005380	-1.81	-1.71421	Copper amine oxidase family protein
Cg9g005370	-1.83	-1.90385	Copper amine oxidase family protein
Cg1g009950	-2.04	-3.01473	calmodulin-binding family protein
Cg4g021370	-2.65	-3.17684	Cadmium/zinc-transporting ATPase HMA2
Cg2g001540	-3.09	-4.80108	Transducin/WD40 repeat-like superfamily protein
Cg2g017030	-3.4	-4.59911	Transducin/WD40 repeat-like superfamily protein
Cg6g016070	-1.13	-1.13584	ABC transporter G family member 34
Nov-m0284-5p	**1.198039**	**1.01773**	
Cg6g016070	-1.13	-1.13584	ABC transporter G family member 34
Cg5g000690	-1.7	undetected	Oligopeptide transporter 7
Cg6g016050	-2.39	-1.89089	ABC transporter G family member 34

RNA	log_2FC(CuR/CKR) by RNAseq	log_2FC(CuR/CKR) by qPCR	*A. thaliana* description
miR166a-5p	**2.37994**	**2.444839**	
TCONS_00025983	-7.16	-3.31462	
TCONS_00034874	-2.3	-2.30161	
TCONS_00036810	-1.92	-1.70539	
Cg2g034240	-1.17	-2.05887	MATE efflux family protein
Cg3g013610	-2.61	-3.0194	Oligopeptide transporter 4
Cg3g013620	-1.5	-1.66687	Oligopeptide transporter 2
Cg5g001820	-1.35	undetected	ABC transporter C family member 10
Cg5g008640	-3.08	-3.69684	Monocopper oxidase-like protein SKU5
Cg5g011170	-1.72	-1.56999	Chaperone protein ClpB1
Cg5g018290	-1.11	-0.16429	ABC transporter G family member 37
Cg6g006410	-2.24	-3.65275	Laccase-4
Cg6g016050	-2.39	-1.89089	ABC transporter G family member 34
Cg6g016070	-1.13	-1.13584	ABC transporter G family member 34
Cg7g005630	-1.6	-1.39821	ABC transporter G family member 6
Cg7g023250	-1.76	-1.79581	E3 ubiquitin ligase BIG BROTHER
Cg8g001210	-1.53	undetected	Major facilitator superfamily protein
Cg9g000380	-1.08	undetected	ABC transporter G family member 37
miR165a-5p	**2.203897**	**2.322514**	
TCONS_00036810	-1.92	-1.70539	
Cg2g013970	-2.75	-2.55165	Laccase-3
Cg3g013430	-1.32	-1.66301	MATE efflux family protein
Cg3g013610	-2.61	-3.01937	Oligopeptide transporter 4
Cg3g013620	-1.5	-1.66687	Oligopeptide transporter 2
Cg3g024660	-1.87	-2.19929	Major facilitator superfamily protein
Cg3g024680	-1.96	-2.62043	Plastocyanin major isoform, chloroplastic
Cg5g011170	-1.72	-1.56999	Chaperone protein ClpB1
Cg5g018290	-1.11	-0.16429	ABC transporter G family member 37
Cg6g016050	-2.39	-1.89089	ABC transporter G family member 34
Cg7g000950	-2.35	-2.44466	Laccase-4
Cg7g023250	-1.76	-1.79581	E3 ubiquitin ligase BIG BROTHER
Cg8g001210	-1.53	undetected	Major facilitator superfamily protein
Cg8g024760	-1.34	-0.91518	Calcineurin-like metallo-phosphoesterase superfamily protein
Cg9g000380	-1.08	undetected	ABC transporter G family member 37

Figures

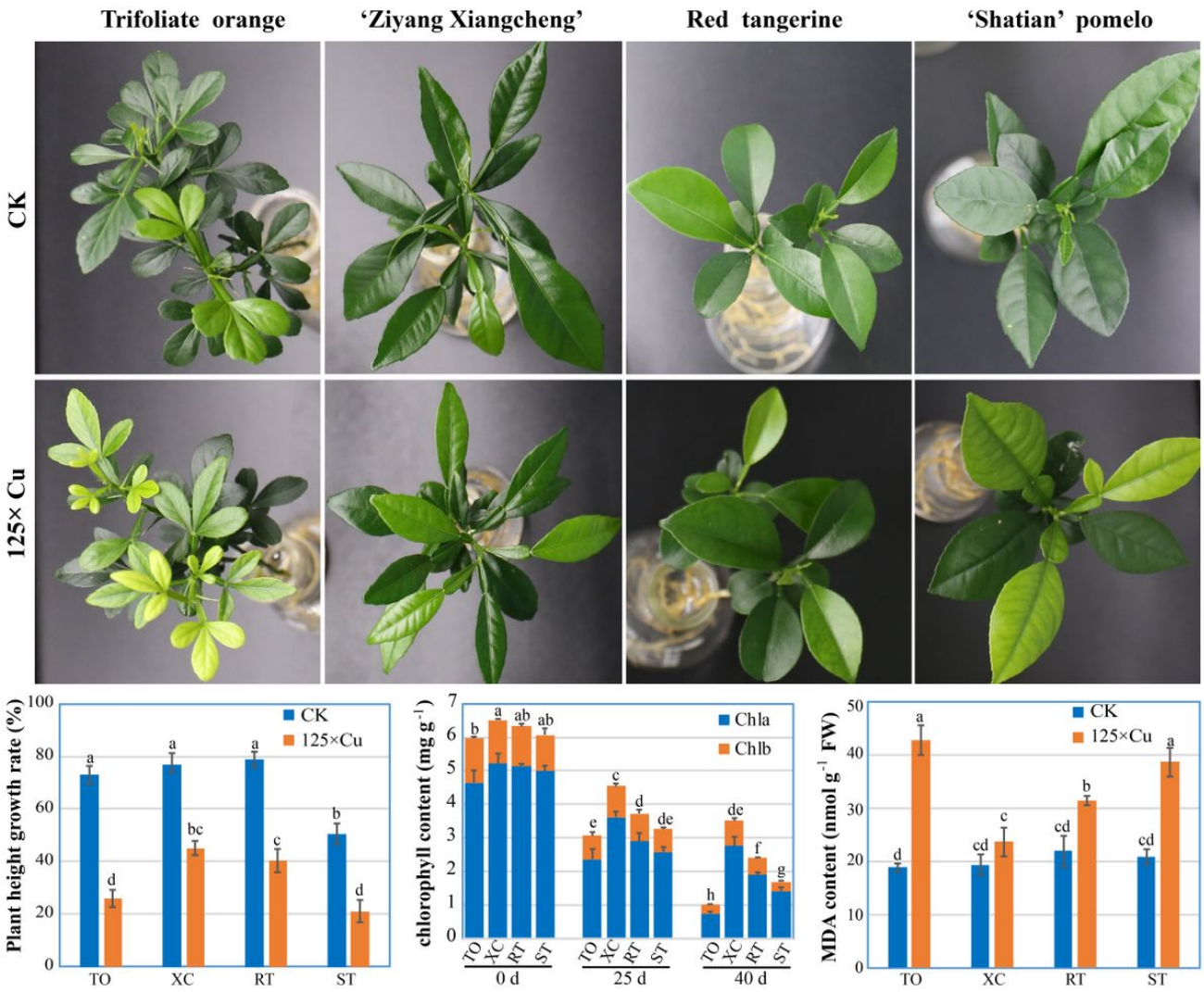

Figure 1

Phenotype and physiological changes of four rootstocks under normal (CK) and Cu toxicity. Four common citrus rootstocks, trifoliate orange (TO), 'Ziyang Xiangcheng' (XC), red tangerine (RT), and 'Shatian' pummelo (ST), were grown under normal and excess of Cu (187.5 μM, 125×) conditions. After 25 d of treatment, representative pictures were photographed. Plant height growth rate and malonaldehyde (MDA) content were determined at 40 d, while chlorophyll a (chla) and b (chlb) contents were measured at 0 d, 25 d, and 40 d. Data are means ± SE (n=3). Different letters indicate significant differences at $P < 0.05$ by Tukey test..

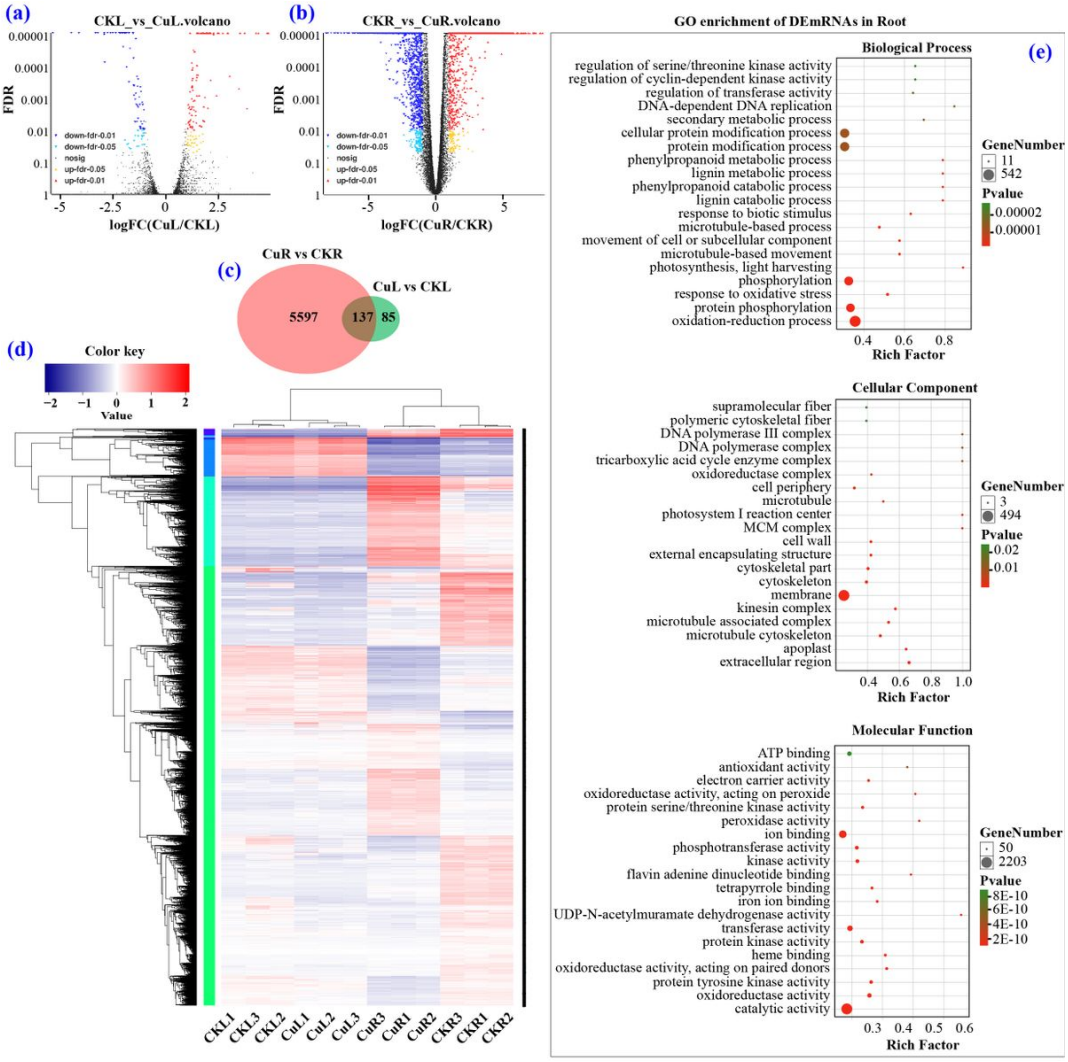

Figure 2

Identification and analysis of differentially expressed mRNAs (DEmRNAs) under Cu toxicity. (a, b) Volcano Plot pictures showing log¬2FC values and FDR of mRNAs in CuL/CKL and CuR/CKR. (c) Venn diagram showing the number of DEmRNAs in CuL/CKL and CuR/CKR. (d) Heat map of all DEmRNAs. (e) GO enrichment of DEmRNAs in the root.

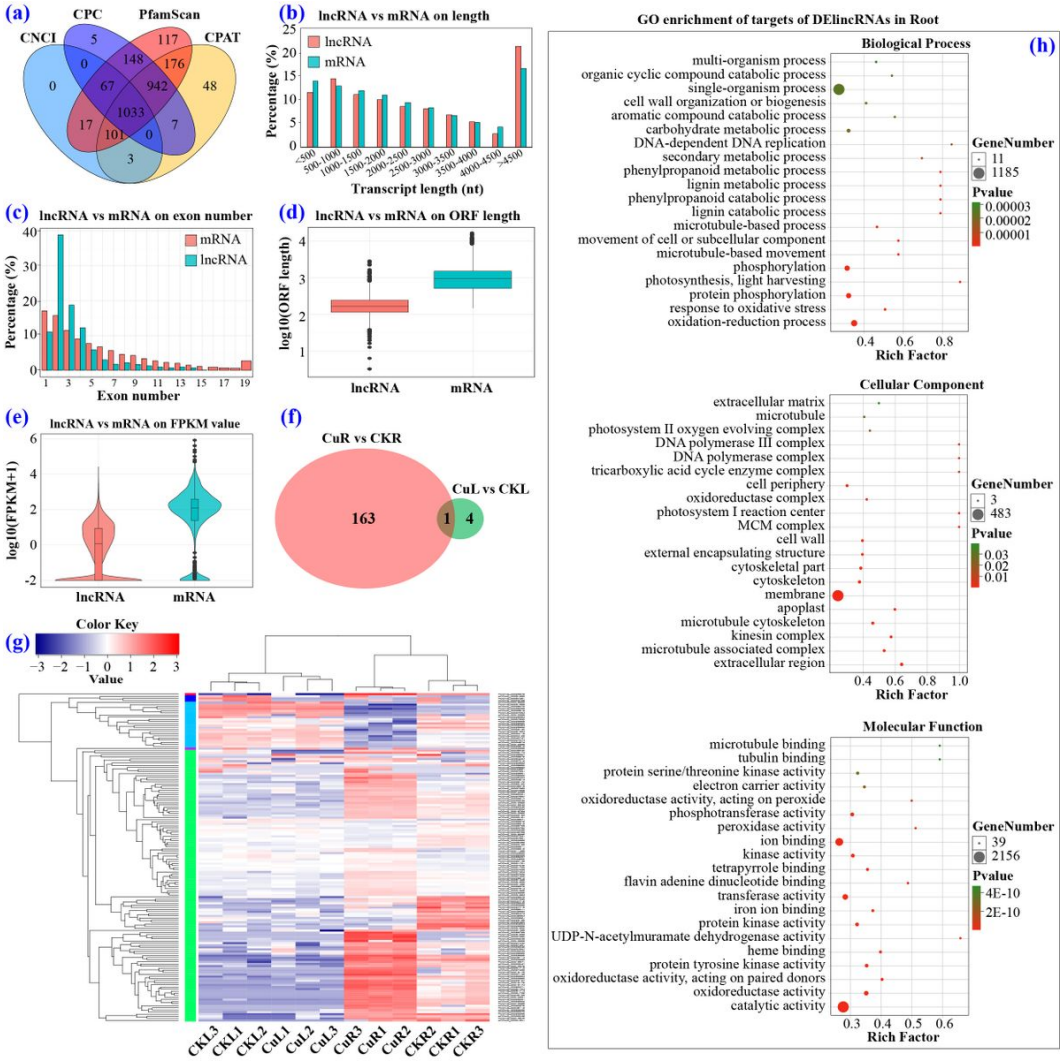

Figure 3

Identification and analysis of differentially expressed lncRNAs (DElncRNAs) under Cu toxicity. (a) Venn diagram showing the number of lncRNAs identified by CNCI, CPC, PfamScan and CPAT methods. (b–e) Comparison of lncRNA with mRNA with respect to the transcript length, exon number, ORF length and FPKM value. (f) Venn diagram showing the number of DElncRNAs in CuL/CKL and CuR/CKR. (g) Heat map of all DElncRNAs. (h) GO enrichment of targets of DElncRNAs in the root.

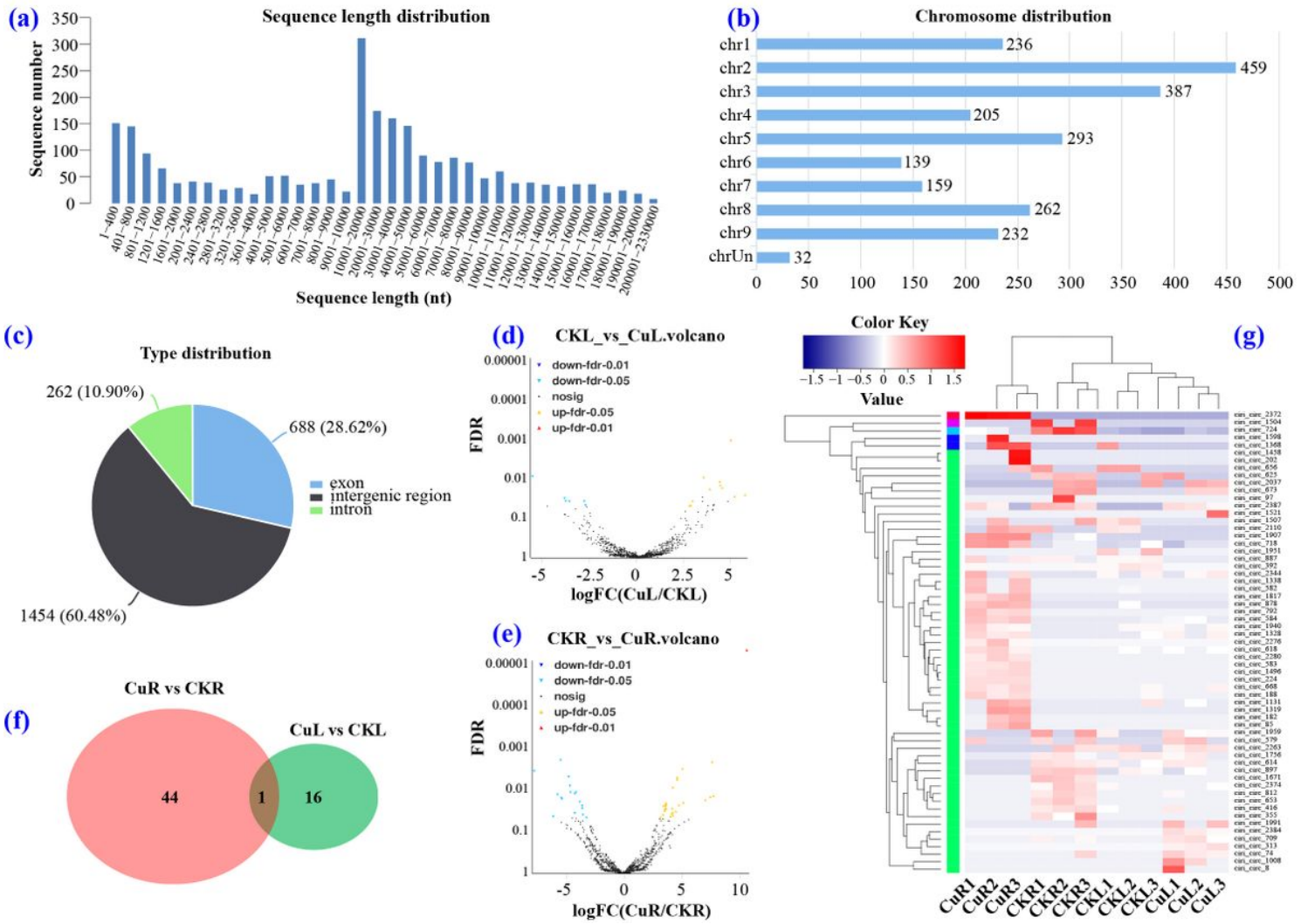

Figure 4

Identification and analysis of differentially expressed circRNAs (DEcircRNAs) under Cu toxicity. (a–c) Sequence length, chromosome, and type distribution of all identified circRNAs. (d, e) Volcano Plot pictures showing log¬2FC values and FDR of circRNAs in CuL/CKL and CuR/CKR. (f) Venn diagram showing the number of DEcircRNAs in CuL/CKL and CuR/CKR. (g) Heat map of all DEcircRNAs.

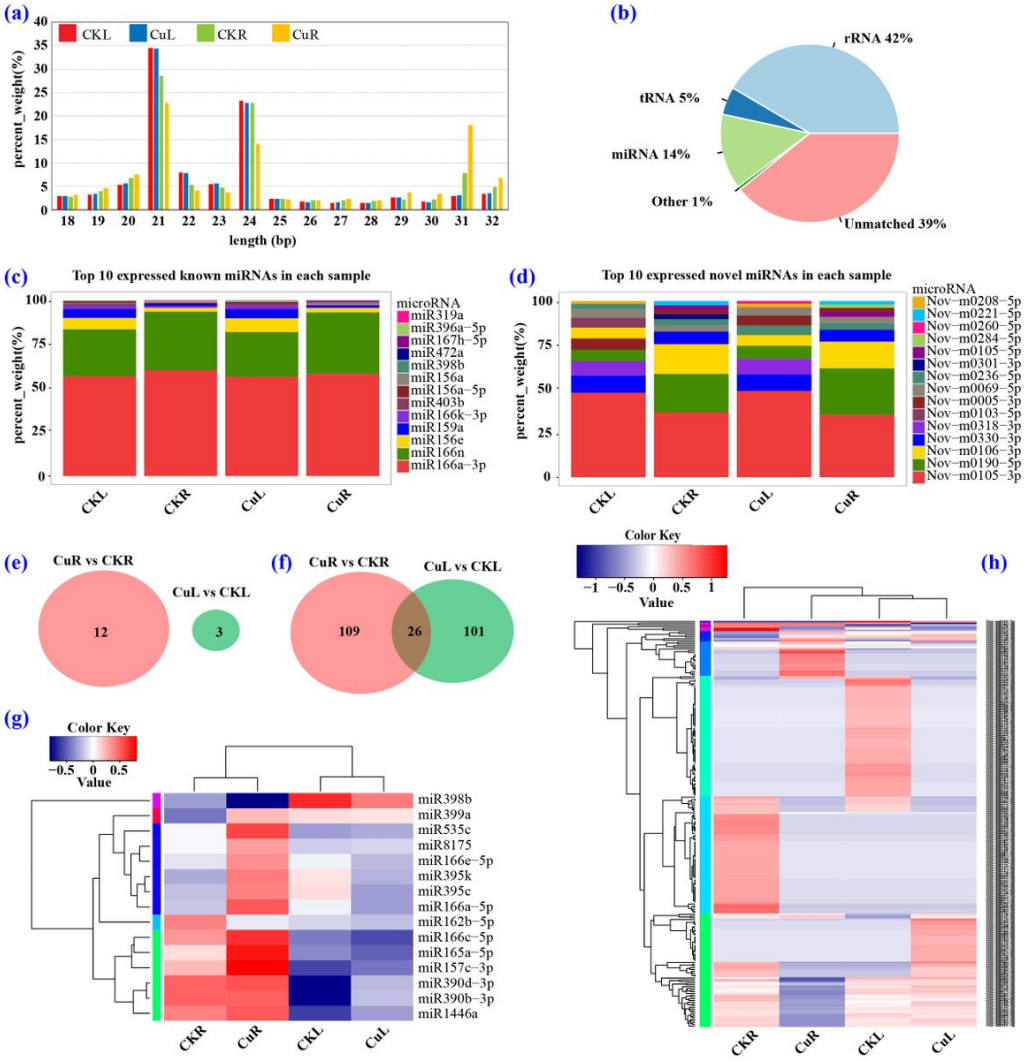

Figure 5

Identification and analysis of differentially expressed miRNAs (DEmiRNAs) under Cu toxicity. (a) Length distribution of all identified small RNAs. (b) Percentage of different types of small RNAs. (c-d) Top 10 expressed known and novel miRNAs in each sample. (e-f) Venn diagram showing the number of known (e) and novel (f) DEmiRNAs in CuL/CKL and CuR/CKR. (g-h) Heat map of all known (g) and novel (h) DEmiRNAs.

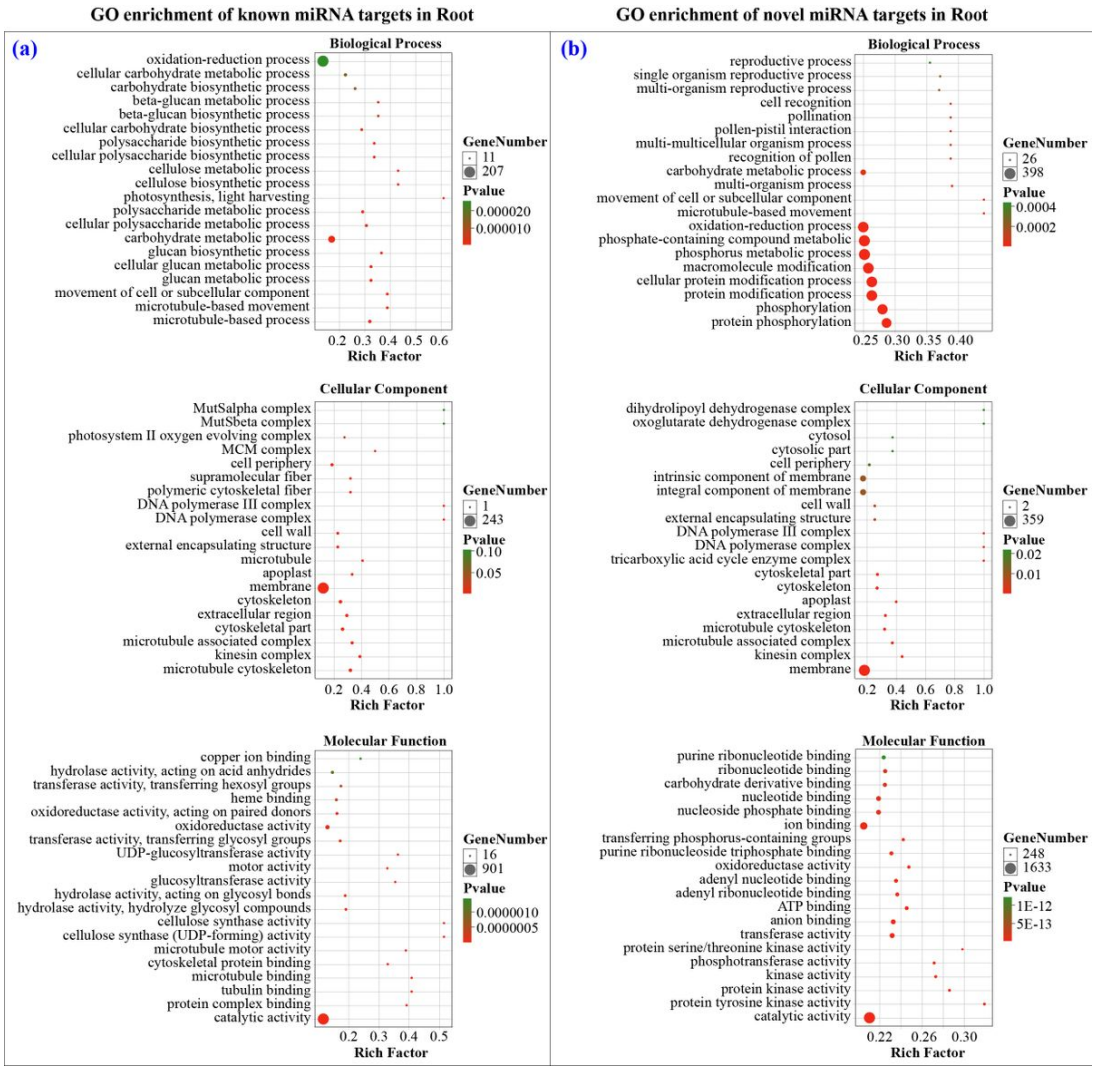

Figure 6

GO enrichment of targets of known (a) and novel (b) DEmiRNAs in the root.

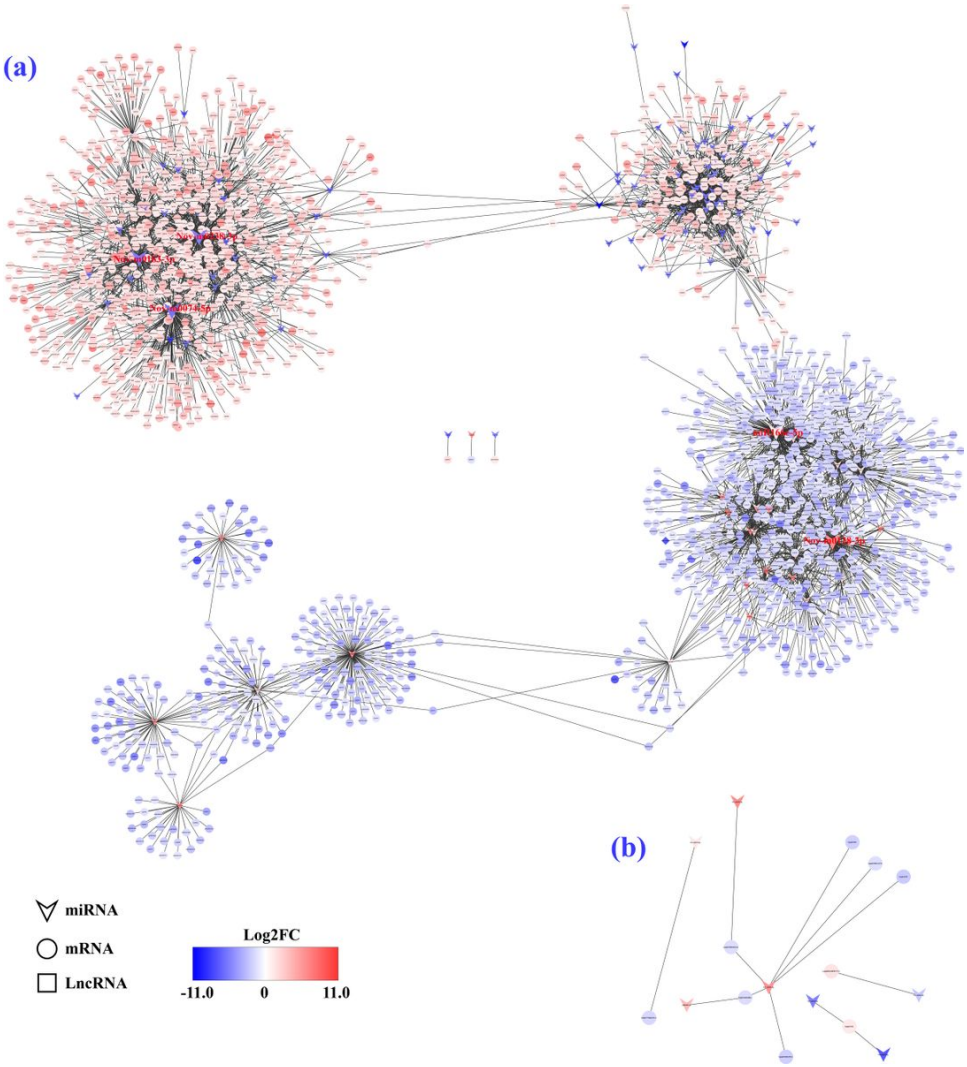

Figure 7

CeRNA network constructed with all DEmRNAs, DElncRNAs and DEmiRNAs in the root (a) and leaf (b). Color represents the up-regulated (red color) and down-regulated (blue color) levels.

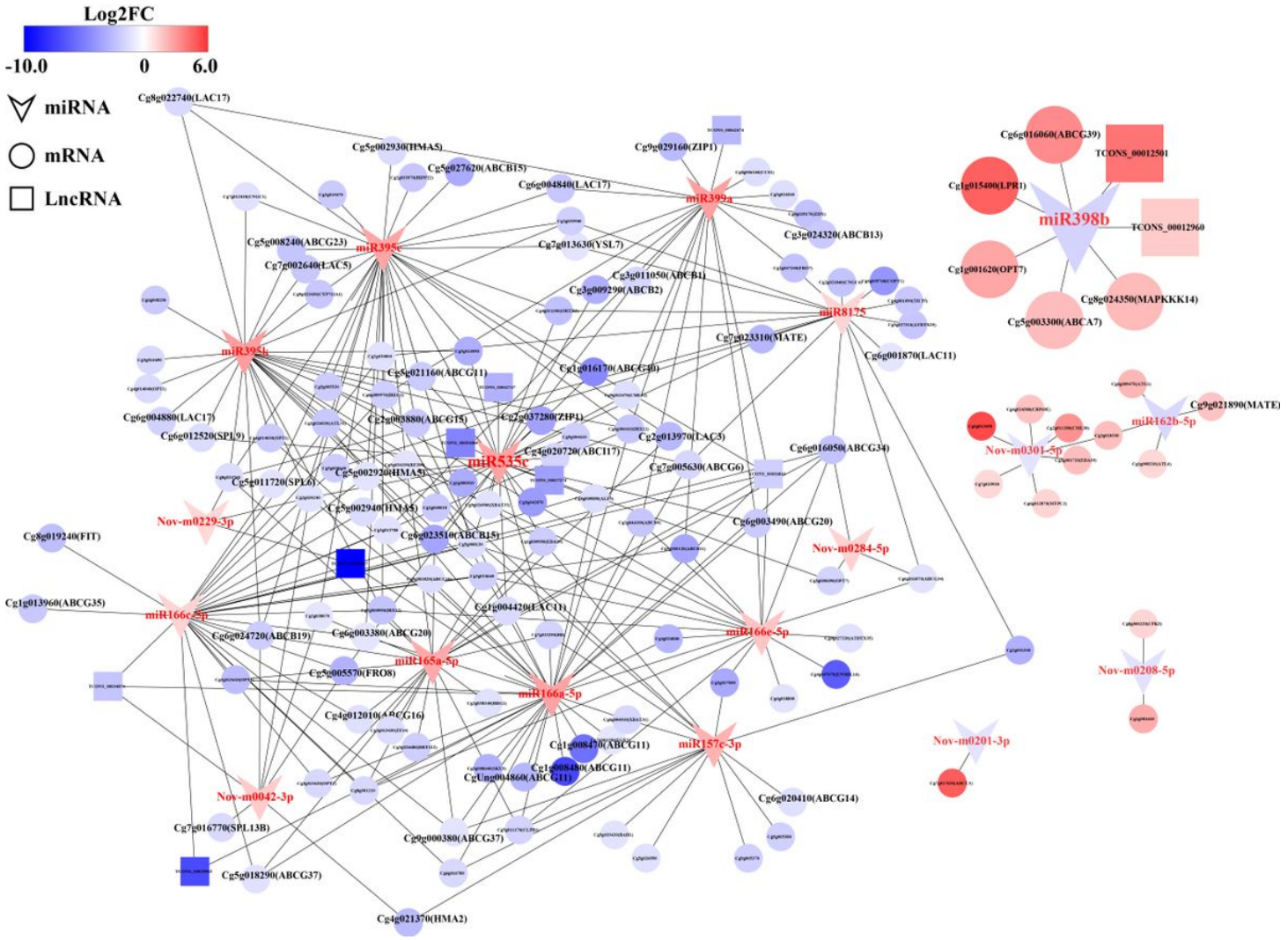

Figure 8

Mini-ceRNA network constructed with 284 known Cu-related DEmRNAs and all DElncRNAs and DEmiRNAs in the root. Color represents the up-regulated (red color) and down-regulated (blue color) levels.

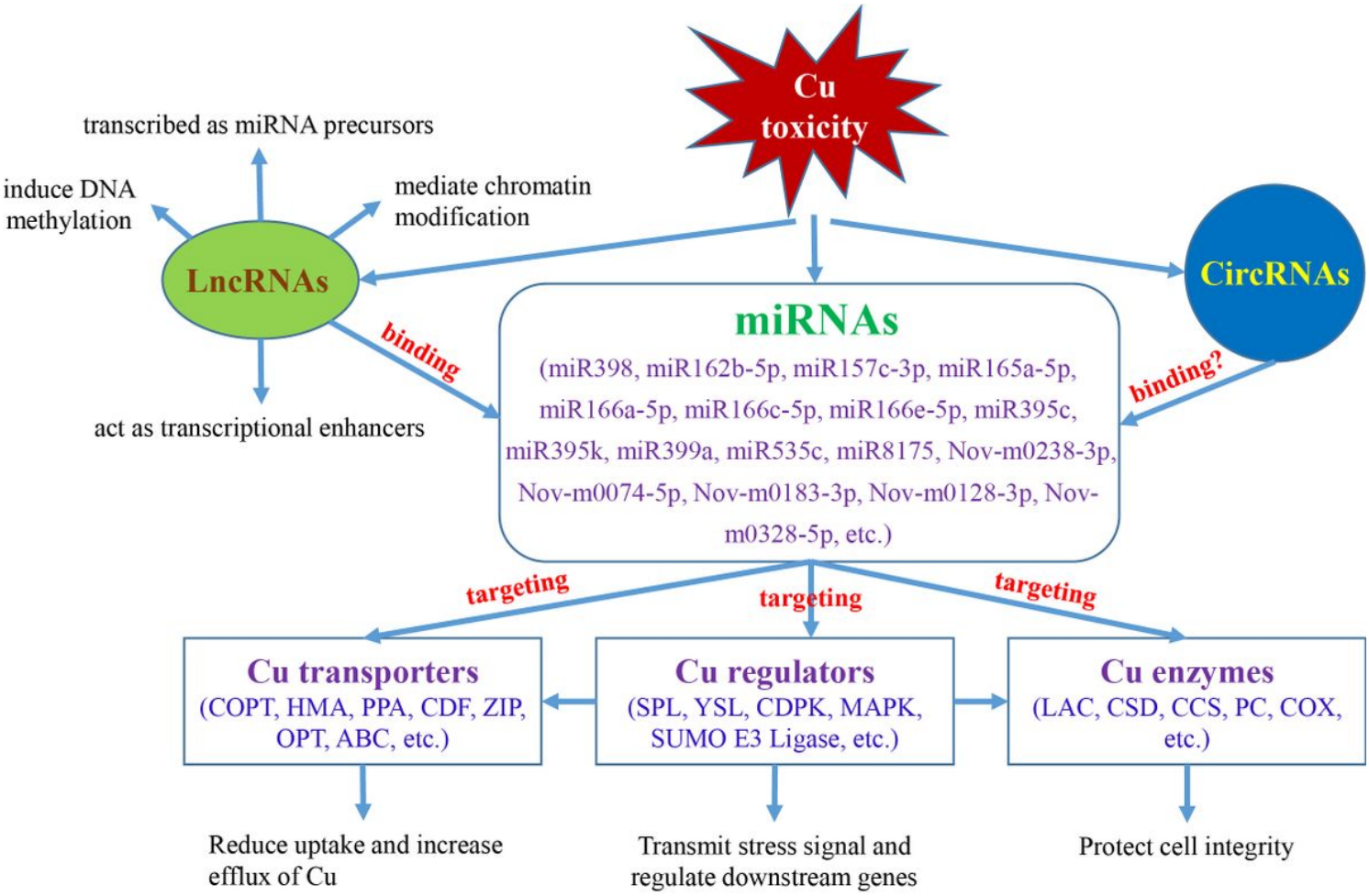

Figure 9

The proposed model in response to Cu toxicity in citrus. Under Cu toxicity, miRNAs act as the key regulators that directly target important Cu transporters, Cu proteins and Cu regulators (TFs and kinases). In this process, some lncRNAs and circRNAs can act as ceRNA to competitively bind the MRE of miRNAs, which may indirectly affect the expression of mRNA.

Supplementary Files

This is a list of supplementary files associated with this preprint. Click to download.

- supplement1.xlsx
- supplement2.xlsx
- supplement3.jpg
- supplement4.jpg
- supplement4.xlsx
- supplement6.xlsx
- supplement7.xlsx
- supplement8.jpg
- supplement9.xlsx
- supplement10.xlsx
- supplement11.xlsx
- supplement12.xlsx